Bulk Metallic Glass Nanowire Architecture for Electrochemical Applications

Marcelo Carmo,[†] Ryan C. Sekol,[†] Shiyan Ding,[‡] Golden Kumar,[‡] Jan Schroers,[‡] and André D. Taylor[†,*]

[†]Chemical & Environmental Engineering Department and [‡]Mechanical Engineering & Materials Science Department, Yale University, New Haven, Connecticut 06511, United States

ABSTRACT Electrochemical devices have the potential to pose powerful solutions in addressing rising energy demands and counteracting environmental problems. However, currently, these devices suffer from meager performance due to poor efficiency and durability of the catalysts. These suboptimal characteristics have hampered widespread commercialization. Here we report on $Pt_{57.5}Cu_{14.7}Ni_{5.3}P_{22.5}$ bulk metallic glass (Pt-BMG) nanowires, whose novel architecture and outstanding durability circumvent the performance problems of electrochemical devices. We fabricate Pt-BMG nanowires using a facile and scalable nanoimprinting approach to create dealloyed high surface area nanowire catalysts with high conductivity and activity for methanol and ethanol oxidation. After 1000 cycles, these nanowires maintain 96% of their performance—2.4 times as much as conventional Pt/C catalysts. Their properties make them ideal candidates for widespread commercial use such as for energy conversion/storage and sensors.

KEYWORDS: bulk metallic glasses · nanowires · electrocatalysts · fuel cells · PEMFC · DAFC

High surface area nanostructures are expected to play a major role in sustainable energy conversion due to their broad applicability. These structures can be tuned for applications spanning solar cells,[1] sensors,[2] batteries,[3] and fuel cells.[4,5] Previous fuel cell catalyst synthesis efforts have focused on the decoration of highly conductive 1-D carbon nanotubes to improve the utilization and dispersion of supported catalysts.[6,7] However, the presence of carbon degrades durability and leads to a fast and significant loss of electrochemical surface area (ECSA) during fuel cell operation.[8] Thus, there has been considerable interest in the development of nanowire fuel cell catalysts.[9,10]

To develop such catalysts, several characteristics have to be taken into consideration for their synthesis and assembly. For fuel cell catalysis, high surface area, multicomponent nanowire alloys are particularly promising for increasing the activity and utilization of precious metals, as seen, for example, for Pt and Pd nanotubes,[5] Au−Ag nanoporous nanotubes,[11] NiCu,[12] and PtCo nanowires.[13] Recently, we also showed that the presence of Ru lowers the susceptibility of Pt from being poisoned from strongly adsorbed intermediate species during the alcohol oxidation reaction.[14] These improvements are due to ensemble effects that arise when dissimilar surface atoms induce electronic charge transfer between the atoms that improve their electronic band structure.[15] Previous nanometallic synthesis efforts have focused on bottom-up assembly through the reduction of salt precursors or electrochemical deposition processes to create nanostructured catalysts. However, these strategies involve complex synthesis methods due to the difficulty in fabricating metallic nanostructures necessary for maintaining high dispersion and noble metal utilization.

Bulk metallic glasses (BMGs) possess many of the desired characteristics. They exist in a wide range of compositions[16] and can be thermoplastically formed (TPF) into complex geometries over a length scale ranging from 10 nm to a few centimeters.[17] The absence of grain boundaries and dislocations in the BMG amorphous structure result in a homogeneous and isotropic material down to the atomic scale, which displays very high strength and elasticity combined with good corrosion resistance.[16]

In this work, we assess the assembly, architecture, and durability of $Pt_{57.5}Cu_{14.7}Ni_{5.3}P_{22.5}$ (atomic %) (Pt-BMG) as an electrochemical device given its excellent formability and large precious metal content.[16] We use a top-down approach employing nanoimprinting[18] to fabricate Pt-BMG nanowires in an economical and scalable way. Our work shows that Pt-BMG properties, composition, and geometry are suitable for high-performance electrocatalysts. Further-

* Address correspondence to andre.taylor@yale.edu.

Received for review January 4, 2011 and accepted February 18, 2011.

Published online March 03, 2011
10.1021/nn200033c

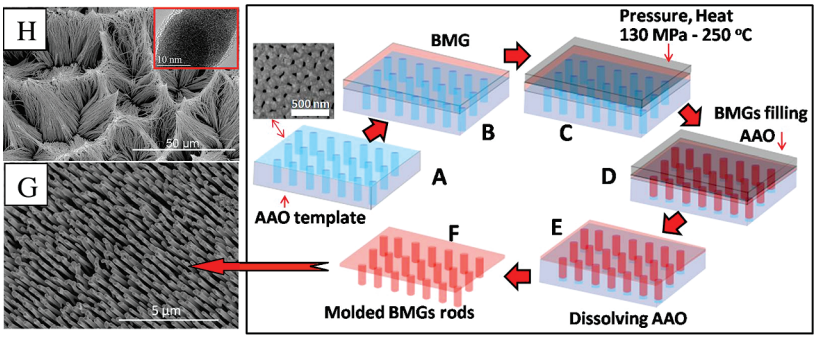

Figure 1. (A−F) Schematic synthesis of Pt-BMG nanowires. (G,H) SEM images of Pt-BMG nanowires; (H, inset) TEM image of Pt-BMG nanowires with a 13 nm diameter.

more, the high level of controllability of Pt-BMG during thermoplastic formation in the highly viscous supercooled liquid region results in high Pt dispersion without the need for a high surface area conductive support (*e.g.*, carbon nanotubes).

RESULTS

To fabricate Pt-BMG nanowires, the Pt-BMG is placed on top of an anodic aluminum oxide (AAO) template and is heated into its supercooled liquid region (see Figure 1 for whole process). Under a low applied pressure (130 MPa), the Pt-BMG fills the nanopores of the AAO template (Figure 1D), which subsequently is dissolved in KOH solution (Figure 1E) to expose the Pt-BMG nanowires. The Pt-BMG nanowires are well-isolated and highly ordered with uniform diameter and length (Figure 1G). The average length and diameter of the Pt-BMG nanowires is approximately 600 and 100 nm, respectively (Figure 1G). This fabrication method is CMOS-compatible and can provide an aspect ratio of up to 50 (Figure 1H) by constant heating through the super cooled liquid as opposed to an isothermal process.

The diameter of the Pt-BMG nanowires is very close to conventional fuel cell supported catalyst particle dimensions and can be easily synthesized with the described method (Figure 1), in contrast to existing complex catalyst synthesis techniques.[19] The structure of the Pt-BMG nanowires was characterized by high-resolution transmission electron microscopy (HRTEM) analysis and establishes that BMG nanowires can be easily obtained in an economic and scalable way through this top-down approach. The diameter of the Pt-BMG nanowires can be made even smaller and is currently limited only by the pore size of the AAO templates.[17] Additional SEM and TEM images can be found in the Supporting Information (S1).

Accelerated fuel cell durability comparisons reveal that the conventional Pt/C catalyst degrades to about 40% of the original electrochemical surface area (ECSA) value after 1000 cycles (Figure 2A,B). The comparisons are based on the voltammetric responses of Pt-BMG nanowire electrocatalyst during slow potential (20 mV s^{-1}) cycles between 0.05 and 1.2 V *vs* RHE (reversible hydrogen electrode) under fuel cell operating temperatures (60 °C). The 60% loss for the Pt/C can be attributed to the agglomeration and dissolution of Pt nanoparticles as well as to carbon support degradation.[5,8] In sharp contrast, the Pt-BMG nanowires maintain their ECSA, displaying an initial ECSA increase followed by a stable plateau at 96% beginning after 300 cycles.

The anodic peak at the initial cycle accounts for the initial increase of ECSA (inset of Figure 2A). To understand this behavior as well as the increase in ECSA during the first cycles (Figure 2A), we carried out X-ray photoelectron spectroscopy (XPS) (Figure 2D−F). Our analysis for Pt-BMG before and after cycling (1000 cycles) at 50 mV s^{-1} reveals that for the Pt 4f region of the Pt spectrum, the most intense doublet (at ~71 and ~74 eV) is characteristic of metallic Pt. There is no indication of a second doublet (at ~72 and ~75 eV), which would be characteristic for oxidized Pt.

The negative shifts in the Pt 4f signal relative to Pt (after 1000 CV cycles) are an indication of electron transfer from the Cu and/or Ni atoms to the neighboring more electronegative Pt atoms.[20] The peak area for the Cu 2p1/2 and 2p3/2 peak decreases after cycling, indicating that the Pt-BMG has an enhanced Pt-rich surface and lower Cu content after cycling (see also Tables S1 and S2 in the Supporting Information). Therefore, consistent with previous work,[21] we can attribute the increase in Pt-BMG nanowire ECSA during the initial cycles to dealloying, which increases the Pt surface area as the Cu near the surface dissolves. For the same reason, the anodic peak indicated by the arrow at 0.3−0.4 V on the initial cycles implies selective Cu dissolution from the Pt-BMG electrode material (Figure 2A, inset).[21] This dealloying effect changes the surface of the Pt-BMG nanowires, leading to a higher activity.[21] The CV stabilizes after 300 cycles, indicating that Cu dissolution from the Pt-BMG surface either ceases or drops to undetectable levels (Figure 2B).

Cyclic voltammetry revealed a dramatic increase in ECSA (beyond the increase in geometric surface area) going from a flat Pt-BMG surface to a nanowire architecture (see also Table S3). This can be explained by the dealloying effect combined with the morphology of

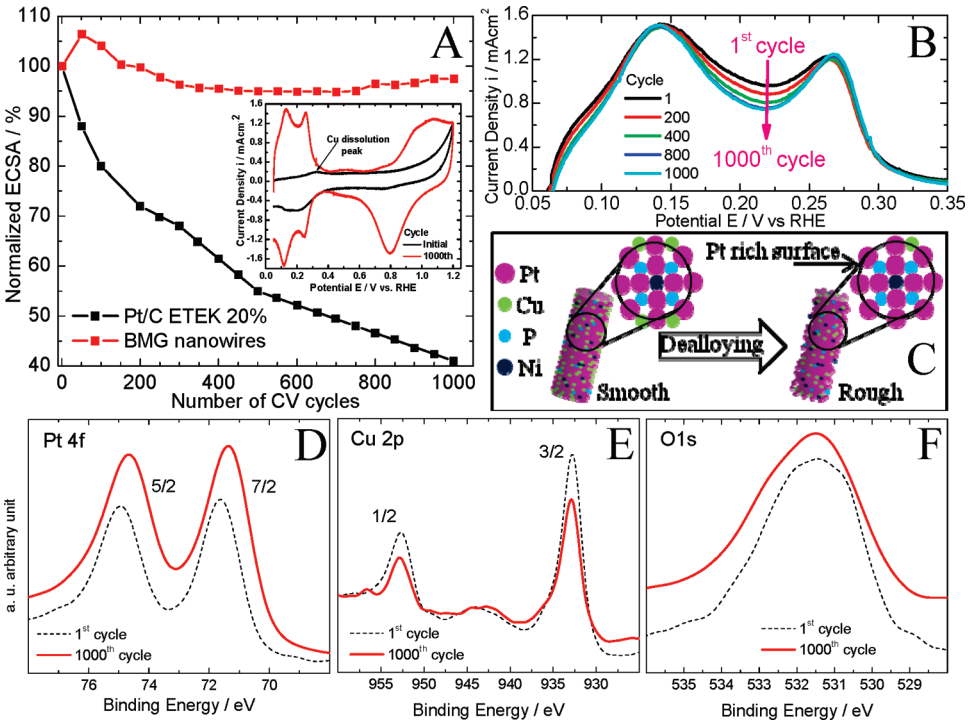

Figure 2. (A) Loss of the electrochemical surface area (ECSA) of Pt-BMG and Pt/C (E-TEK) catalysts with the number of cyclic voltammogram (CV) cycles in nitrogen-purged 0.5 mol L^{-1} H_2SO_4 solution, at 60 °C. Inset: Cyclic voltammograms (initial and after 1000 cycles) of Pt-BMG nanowire catalysts. (B) Hydrogen under potential deposition region from the cyclic voltammograms used for measuring the ECSA of Pt-BMG catalysts at 60 °C from 0 to 1000 cycles. The CVs were recorded in N_2-saturated 0.5 M H_2SO_4 solution at room temperature. Scan rate: 20 mV/s. (C) Schematic representation of structural changes of Pt-BMG nanowires as a result of the electrochemical dealloying effect. X-ray photoelectron spectroscopy spectra for (D) Pt 4f5/2, 4f7/2, (E) Cu2p1/2, 2p3/2, and (F) O1s, performed on the Pt-BMG electrode before and after 1000 CV cycles (durability test). The deconvoluted data are presented in Tables S1 and S2 in the Supporting Information.

the electrodes. Although dealloying is a beneficial effect for the BMG nanowire architecture, it has been used previously by itself to produce effective large surface area architectures with high activities.[21] This is achieved through preferential dissolution, removal, or spinodal decomposition of bimetallic alloys where the less noble atom (*i.e.*, Cu) is dissolved while the more noble metal atoms (*i.e.*, Pt) remain as a porous skeleton of the more noble metal component. Chen *et al.*, who reported an enhanced durability for pure Pt nanotubes (PtNTs), suggested that the activity of the PtNTs could be further improved by employing Pt alloy nanotubes.[5] In contrast to the highly complex synthesis, low throughput, low reproducibility, and high cost typically associated with conventional nanostructure fabrication,[19,22] this architectural approach can be realized easily with our top-down approach for the fabrication of the Pt-BMG nanowire.

A key limiting factor for direct methanol and ethanol fuel cell catalysts is intermediate species (*i.e.*, CO) generated during the reaction. Such intermediates can strongly adsorb onto the surface of the noble metal, resulting in low power densities.[23] The oxidation of a monolayer of CO onto a conventional flat pure Pt disk (labeled as Pt flat) and Pt-BMG surfaces (flat and nanowire arrays with diameters of 13−100 nm and an average length of 600 nm) is shown in Figure 3A. In each case, at the beginning of the first sweep, CO blocks the Pt sites with no hydrogen oxidation observed at low potential. The Pt-BMG nanowires, however, have an enhanced CO_{ads} tolerance which contributes to a lower onset potential for CO oxidation (~0.4 V *vs* RHE) compared to pure Pt (~0.8 V *vs* RHE) (Figure 3A, inset). As a result, Pt-BMG nanowires are less susceptible to self-poisoning (due to CO generation from the alcohol electrochemical oxidation step) than pure Pt (Figure 3B,C). Remarkably, higher alcohol oxidation current densities are present for the Pt-BMG nanowires with 13 nm in diameter than for the other electrodes. Additional chronoamperometry profiles for methanol and ethanol oxidation can be found in the Supporting Information (S2).

Electronic and strain effects may play a major role in the activity enhancement for carbon monoxide, methanol, and ethanol oxidation.[24] Alloying Pt with other metals can lower the electronic binding energy in Pt and promote the C−H cleavage reaction at low potential.[24] Strains that widely exist in the dealloyed materials have also been demonstrated to be favorable for the enhancement of electrocatalytic activity in Pt-based alloys.[21] Our results suggest that the enhanced activity for the methanol and ethanol oxidation of Pt-BMGs compared to pure Pt can be ascribed to the synergetic effect of Ni and any remaining Cu. These interactions promote the formation of hydroxyl species by dissociating water at a lower potential with respect

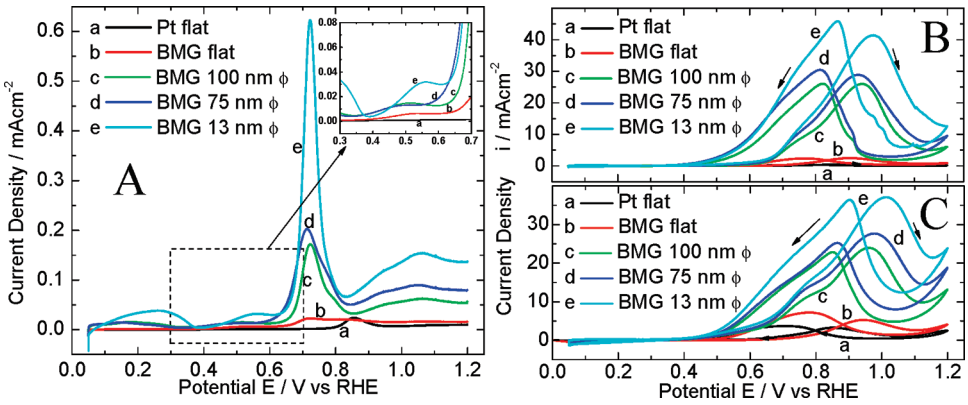

Figure 3. Electrocatalytic performance of the Pt-BMG nanowires toward (A) carbon monoxide (CO) oxidation, (B) methanol 1 mol L^{-1} oxidation, and (C) ethanol 1 mol L^{-1}oxidation. Cyclic voltammograms in 0.5 mol L^{-1} H_2SO_4, normalized to the electrode geometric area. Scan rate: 20 mV s^{-1}.

to the pure Pt catalysts. Moreover, such interactions could also weaken the bonding between the hydroxyl species and the catalyst surface for Pt-BMGs compared to the bonding on conventional Pt catalysts. The more weakly adsorbed hydroxyl species further promote the electro-oxidation of adsorbed CO and/or methanol/ethanol subproduct species on the active metal sites at low potentials, thus improving the performance.[14]

Our results suggest that composition and geometry play a key role in the observed enhanced catalytic activity of Pt-BMG nanowires with respect to methanol and ethanol oxidation. The oxidation of organic molecules involves a multistep adsorption and electron transfer, requiring multiple adjacent active Pt sites.[24] The unique features of the Pt-enriched surface of the Pt-BMG nanowires through Cu dissolution render the surface favorable for the oxidation of methanol and ethanol. The Pt-enriched nature of the outer surface enables all surface sites of the BMG nanowires to be highly conductive. Electrons produced on the surfaces of the BMGs can flow across the catalyst without encountering any significant ohmic barriers. Therefore, the high intrinsic electrical conductivity of the Pt-BMGs might also contribute to their high performance. This conductivity augments the reaction kinetics on the catalyst surfaces and hence may result in an enhancement in activity.[25] The search for higher conductive materials is a highly pursued area, starting from carbon blacks, carbon nanofibers,[26] carbon nanotubes,[14] and graphene[27] materials. Pt-BMG conductivity (0.32×10^6 S m^{-1}) exceeds that of carbon black (0.001−0.01 S m^{-1})[28] by 4 orders of magnitude and that of carbon nanotubes by 1 order of magnitude (0.025×10^6 S m^{-1}).[29]

In summary, Pt-BMG nanowire architecture exhibits superb durability combined with high electrocatalytic activity toward CO, methanol, and ethanol oxidation. The demonstrated performance suggests widespread commercial use and applicability, which is easy, scalable, and economical in fabrication. Developing specifically tailored alloys of BMGs for electrocatalytic applications could result in transformative improvements in a multitude of areas such as energy conversion/storage and sensors.

METHODS

The preparation of $Pt_{57.5}Cu_{14.7}Ni_{5.3}P_{22.5}$ bulk metallic glass used here is described in detail in previous papers.[16] Briefly, alloying of high-purity constituents was carried out in an arc melter under an argon atmosphere. Subsequently, the alloys were processed in quartz tubes with an inner diameter of 12 mm and vitrified by water quenching from a temperature of 1000 °C, 250 °C above the thermodynamic liquids temperature. The parameters for thermoplastic forming experiments were selected on the basis of the crystallization and viscosity data of the metallic glasses. Commercially available nanoporous anodized aluminum oxide (AAO) molds were used as a template for nanomolding in this work. For the molding of very high aspect ratio nanostructures, the metallic glass was thermoplastically formed from T_g to T_x (where T_x is the onset of crystallization) under a constant load of 130 MPa. The metallic glass nanowires were released from the AAO template by etching with KOH solution.

Transmission electron microscopy (TEM) was carried out on a JEOL 3010 HREM instrument operating at 300 kV. Scanning electron microscopy (SEM) was conducted on a PHILIPS XL30-FEG instrument at 10 kV.

The XPS measurements were performed using a VSW Scientific Instruments (Manchester, England) apparatus; the X-ray source was Al Kα at a power of 150 W. Spectra were obtained with pass energy of 15 eV. All of the spectra were obtained in an ion-pumped ultrahigh vacuum (UHV) chamber with a background pressure of around 1×10^{-9} Torr. Samples were mounted on a molybdenum base plate with ceramic bars holding them in. Samples were introduced into the UHV chamber through a differentially pumped fast entry chamber. The peak locations and peak widths were obtained by fitting the data to mixed Gaussian−Lorentzian peak shapes. Prior to fitting, a Shirley background was subtracted from the data using CASA XPS software. The quantitative evaluation of each peak was obtained by dividing the integrated peak area by atomic sensitivity factors of each element.

The electrochemical measurements were conducted in an electrochemical cell from PINE Instruments using a homemade rotating disk electrode (RDE) set up with a multichannel

potentiostat (Biologic Instruments) and rotation control (AFR, Pine Instruments). Potentials were determined using a reversible hydrogen reference electrode (RHE) that was separated from the working electrode compartment by a closed electrolyte bridge. The cyclic voltammetry (CV) test for accelerated durability was performed on the working electrode by cycling the voltage between 0.05 and 1.2 V *versus* RHE in nitrogen purged 0.5 mol L^{-1} aqueous H_2SO_4 solution at room temperature (~25 °C) or 60 °C. The scan rate was 50 mV s^{-1}. The electrochemical surface areas (ECSA) were calculated based on our previous work.[14] Briefly, it was calculated from the H_2 desorption peak of the CV cycle, from the Coulombic charge for hydrogen desorption, assuming a value of 220 μCcm^{-2} Pt for the oxidation of adsorbed atomic hydrogen on a smooth Pt surface. For ECSA evaluated using CO-stripping voltammetry, a charge of 420 μCcm^{-2} on a smooth Pt surface was used.

Acknowledgment. We gratefully acknowledge M. W. Herdiech and E. I. Altman (Yale University) for the XPS measurement. J.S. would like to acknowledge funding from Yale University's Center for Research on Interface Structures and Phenomena (CRISP) and NSF-NM#CMMI-0928227. A.D.T. would like to acknowledge funding from NSF-CBET-0954985 CAREER Award.

Supporting Information Available: Additional SEM and TEM pictures, XPS supporting data, electrochemical surface area (ECSA), and chronoamperometry data for the prepared materials. This material is available free of charge *via* the Internet at http://pubs.acs.org.

REFERENCES AND NOTES

1. Law, M.; Greene, L. E.; Johnson, J. C.; Saykally, R.; Yang, P. D. Nanowire Dye-Sensitized Solar Cells. *Nat. Mater.* **2005,** *4*, 455–459.
2. Wan, Q.; Li, Q. H.; Chen, Y. J.; Wang, T. H.; He, X. L.; Li, J. P.; Lin, C. L. Fabrication and Ethanol Sensing Characteristics of ZnO Nanowire Gas Sensors. *Appl. Phys. Lett.* **2004,** *84*, 3654–3656.
3. Chan, C. K.; Patel, R. N.; O'Connell, M. J.; Korgel, B. A.; Cui, Y. Solution-Grown Silicon Nanowires for Lithium-Ion Battery Anodes. *ACS Nano* **2010,** *4*, 1443–1450.
4. Bell, A. T. The Impact of Nanoscience on Heterogeneous Catalysis. *Science* **2003,** *299*, 1688–1691.
5. Chen, Z. W.; Waje, M.; Li, W. Z.; Yan, Y. S. Supportless Pt and PtPd Nanotubes as Electrocatalysts for Oxygen-Reduction Reactions. *Angew. Chem., Int. Ed.* **2007,** *46*, 4060–4063.
6. Taylor, A. D.; Sekol, R. C.; Kizuka, J. M.; D'Cunha, S.; Comisar, C. M. Fuel Cell Performance and Characterization of 1-D Carbon-Supported Platinum Nanocomposites Synthesized in Supercritical Fluids. *J. Catal.* **2008,** *259*, 5–16.
7. Taylor, A. D.; Michel, M.; Sekol, R. C.; Kizuka, J. M.; Kotov, N. A.; Thompson, L. T. Fuel Cell Membrane Electrode Assemblies Fabricated by Layer-by-Layer Electrostatic Self-Assembly Techniques (vol 18, pg 3003, 2008). *Adv. Funct. Mater.* **2008,** *18*, 3354–3354.
8. Ferreira, P. J.; La, O, G. J.; Shao-Horn, Y.; Morgan, D.; Makharia, R.; Kocha, S.; Gasteiger, H. A. Instability of Pt/C Electrocatalysts in Proton Exchange Membrane Fuel Cells—A Mechanistic Investigation. *J. Electrochem. Soc.* **2005,** *152*, A2256–A2271.
9. Xu, C. W.; Wang, H.; Shen, P. K.; Jiang, S. P. Highly Ordered Pd Nanowire Arrays as Effective Electrocatalysts for Ethanol Oxidation in Direct Alcohol Fuel Cells. *Adv. Mater.* **2007,** *19*, 4256–4258.
10. Pan, C. F.; Wu, H.; Wang, C.; Wang, B.; Zhang, L.; Cheng, Z. D.; Hu, P.; Pan, W.; Zhou, Z. Y.; Yang, X.;*et al.*Nanowire-Based High Performance "Micro Fuel Cell": One Nanowire, One Fuel Cell. *Adv. Mater.* **2008,** *20*, 1644–1647.
11. Gu, X. H.; Xu, L. Q.; Tian, F.; Ding, Y. Au−Ag Alloy Nanoporous Nanotubes. *Nano Res.* **2009,** *2*, 386–393.
12. Tian, X. K.; Zhao, X. Y.; Zhang, L. D.; Yang, C.; Pi, Z. B.; Zhang, S. X. Performance of Ethanol Electro-oxidation on Ni−Cu Alloy Nanowires through Composition Modulation. *Nanotechnology* **2008,** *19*, 215711.
13. Liu, L.; Pippel, E.; Scholz, R.; Gosele, U. Nanoporous Pt−Co Alloy Nanowires: Fabrication, Characterization, and Electrocatalytic Properties. *Nano Lett.* **2009,** *9*, 4352–4358.
14. Carmo, M.; Paganin, V. A.; Rosolen, J. M.; Gonzalez, E. R. Alternative Supports for the Preparation of Catalysts for Low-Temperature Fuel Cells: The Use of Carbon Nanotubes. *J. Power Sources* **2005,** *142*, 169–176.
15. Strasser, P.; Koh, S.; Anniyev, T.; Greeley, J.; More, K.; Yu, C.; Liu, Z.; Kaya, S.; Nordlund, D.; Ogasawara, H.;*et al.*Lattice-Strain Control of the Activity in Dealloyed Core−Shell Fuel Cell Catalysts. *Nat. Chem.* **2010,** *2*, 454–460.
16. Schroers, J. Processing of Bulk Metallic Glass. *Adv. Mater.* **2010,** *22*, 1566–1597.
17. Kumar, G.; Tang, H. X.; Schroers, J. Nanomoulding with Amorphous Metals. *Nature* **2009,** *457*, 868–872.
18. Taylor, A.; Lucas, B. D.; Guo, L. J.; Thompson, L. T. Nanoimprinted Electrodes for Micro-Fuel Cell Applications. *J. Power Sources* **2007,** *171*, 218–223.
19. Schmidt, V.; Gosele, U. How Nanowires Grow. *Science* **2007,** *316*, 698–699.
20. Liu, F.; Lee, J. Y.; Zhou, W. J. Segmented Pt/Ru, Pt/Ni, and Pt/RuNi Nanorods as Model Bifunctional Catalysts for Methanol Oxidation. *Small* **2006,** *2*, 121–128.
21. Mani, P.; Srivastava, R.; Strasser, P. Dealloyed Pt−Cu Core−Shell Nanoparticle Electrocatalysts for Use in PEM Fuel Cell Cathodes. *J. Phys. Chem. C* **2008,** *112*, 2770–2778.
22. Fasol, G. Nanowires: Small Is Beautiful. *Science* **1998,** *280*, 545–546.
23. Reddington, E.; Sapienza, A.; Gurau, B.; Viswanathan, R.; Sarangapani, S.; Smotkin, E. S.; Mallouk, T. E. Combinatorial Electrochemistry: A Highly Parallel, Optical Screening Method for Discovery of Better Electrocatalysts. *Science* **1998,** *280*, 1735–1737.
24. Antolini, E.; Salgado, J. R. C.; Gonzalez, E. R. The Methanol Oxidation Reaction on Platinum Alloys with the First Row Transition Metals—The Case of Pt−Co and Pt−Ni Alloy Electrocatalysts for DMFCs: A Short Review. *Appl. Catal. B* **2006,** *63*, 137–149.
25. Xu, C.; Wang, L.; Wang, R.; Wang, K.; Zhang, Y.; Tian, F.; Ding, Y. Nanotubular Mesoporous Bimetallic Nanostructures with Enhanced Electrocatalytic Performance. *Adv. Mater.* **2009,** *21*, 2165–2169.
26. Zaragoza-Martín, F.; Sopeña-Escario, D.; Morallón, E.; de Lecea, C. S.-M. Pt/Carbon Nanofibers Electrocatalysts for Fuel Cells: Effect of the Support Oxidizing Treatment. *J. Power Sources* **2007,** *171*, 302–309.
27. Li, Y.; Tang, L.; Li, J. Preparation and Electrochemical Performance for Methanol Oxidation of Pt/Graphene Nanocomposites. *Electrochem. Commun.* **2009,** *11*, 846–849.
28. Pantea, D.; Darmstadt, H.; Kaliaguine, S.; Roy, C. Electrical Conductivity of Conductive Carbon Blacks: Influence of Surface Chemistry and Topology. *Appl. Surf. Sci.* **2003,** *217*, 181–193.
29. Ebbesen, T. W.; Lezec, H. J.; Hiura, H.; Bennett, J. W.; Ghaemi, H. F.; Thio, T. Electrical Conductivity of Individual Carbon Nanotubes. *Nature* **1996,** *382*, 54–56.